Inorg. Chem. **2005**, *44*, 3112–3120

Esterase-Activated Two-Fluorophore System for Ratiometric Sensing of Biological Zinc(II)

Carolyn C. Woodroofe, Annie C. Won, and Stephen J. Lippard*

Department of Chemistry, Massachusetts Institute of Technology, Cambridge, Massachusetts 02139

Received August 31, 2004

Intracellular ester hydrolysis by cytosolic esterases is a common strategy used to trap fluorescent sensors within the cell. We have prepared analogues of Zinpyr-1 (ZP1), an intensity-based fluorescent sensor for Zn^{2+}, that are linked via an amido-ester or diester moiety to a calibrating fluorophore, coumarin 343. These compounds, designated Coumazin-1 and -2, are nonpolar and are quenched by intramolecular interactions between the two fluorophores. Esterase-catalyzed hydrolysis generates a Zn^{2+}-sensitive ZP1-like fluorophore and a Zn^{2+}-insensitive coumarin as a calibrating fluorophore. Upon excitation of the fluorophores, coumarin 343 emission relays information concerning sensor concentration whereas ZP1 emission indicates the relative concentration of Zn^{2+}-bound sensor. This approach enables intracellular monitoring of total sensor concentration and provides a ratiometric system for sensing biological zinc ion.

Introduction

Divalent zinc plays many important roles in biology.[1] Zn^{2+} is the second most abundant metal in the body and is a structural or catalytic component of more than 300 enzymes. Intracellular concentrations of free Zn^{2+} are closely controlled by a complex and effective system of zinc transporters and zinc-specific solute carriers,[2,3] such that the free or loosely bound Zn^{2+} concentration in the cytosol is subfemtomolar.[4] Much higher cytosolic concentrations of free Zn^{2+} are observed in cells that have undergone oxidative stress.[5]

The synaptic vesicles in the mossy fibers of mammalian hippocampus are of interest because accumulation of loosely bound Zn^{2+}, up to 0.3 mM in concentration, occurs in these intracellular compartments.[6,7] An overriding justification for the entropic cost of this system has not been determined, in part because of the lack of an intrinsic spectroscopic signature with which to study Zn^{2+} and its physiological roles. The development of fluorescent sensors for loosely bound Zn^{2+} is thus of interest in elucidating its movements and functions.

The application of fluorescent sensors to biological systems has traditionally been complicated by an inability to assess the local concentration of the probe. A localized bright fluorescent signal may reflect a large amount of analyte in that area, or it may be an artifact of high local dye concentration. Ratiometric sensors that display two distinctly different measurable signals in the presence and absence of analyte are thus of great interest and utility because they can eliminate such ambiguities.[8]

Several ratiometric fluorescent probes for biological zinc(II) ion have recently been described. The majority of these are based on fluorophores requiring relatively short-wavelength, high-energy excitation sources, such as 2-aryl benzimidazoles,[9] benzoxazoles,[10] and indoles and benzofurans.[11,12] Binding of Zn^{2+} affords a wavelength shift in excitation or emission, based on interruption of fluorophore conjugation or on excited-state intramolecular proton transfer (ESIPT). Excitation wavelengths for these probes range from about 300 to 380 nm, and emission wavelengths vary

* To whom correspondence should be addressed. E-mail: lippard@mit.edu.

(1) Vallee, B. L.; Falchuk, K. H. *Physiol. Rev.* **1993**, *73*, 79−118.
(2) Palmiter, R. D.; Huang, L. *Pflugers Arch.−Eur. J. Physiol.* **2004**, *447*, 744−751.
(3) Kambe, T.; Yamaguchi-Iwai, Y.; Sasaki, R.; Nagao, M. *Cell. Mol. Life Sci.* **2004**, *61*, 49−68.
(4) Outten, C. E.; O'Halloran, T. V. *Science* **2001**, *292*, 2488−2492.
(5) Chang, C. J.; Jaworski, J.; Nolan, E. M.; Sheng, M.; Lippard, S. J. *Proc. Natl. Acad. Sci. U.S.A.* **2004**, *101*, 1129−1134.
(6) Frederickson, C. J. *Int. Rev. Neurobiol.* **1989**, *31*, 145−238.
(7) Frederickson, C. J.; Suh, S. W.; Silva, D.; Frederickson, C. J.; Thompson, R. B. *J. Nutr.* **2000**, *130*, 1471S−1483S.
(8) Tsien, R. Y.; Poenie, M. *Trends Biochem. Sci.* **1986**, *11*, 450−455.
(9) Henary, M. M.; Wu, Y.; Fahrni, C. J. *Chem. Eur. J.* **2004**, *10*, 3015−3025.
(10) Taki, M.; Wolford, J. L.; O'Halloran, T. V. *J. Am. Chem. Soc.* **2004**, *126*, 712−713.
(11) Gee, K. R.; Zhou, Z. L.; Ton-That, D.; Sensi, S. L.; Weiss, J. H. *Cell Calcium* **2002**, *31*, 245−251.
(12) Maruyama, S.; Kikuchi, K.; Hirano, T.; Urano, Y.; Nagano, T. *J. Am. Chem. Soc.* **2002**, *124*, 10650−10651.

10.1021/ic048789s CCC: $30.25
Published on Web 03/31/2005

Scheme 1. Proposed Mechanism of Ratiometric Zn^{2+} Sensing

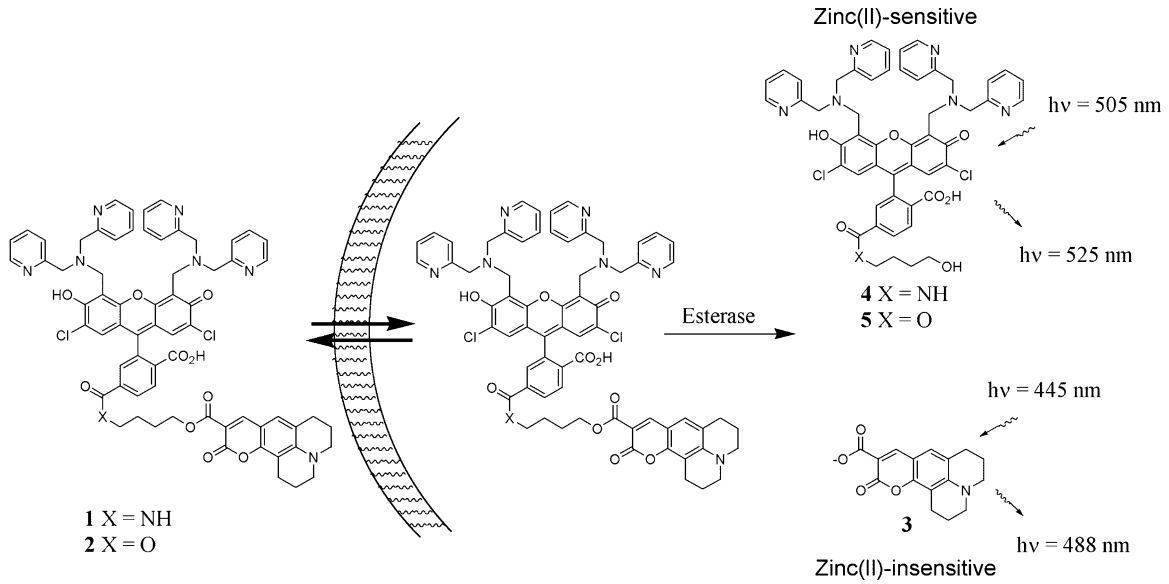

between 395 and 532 nm. ZNP-1, a ratiometric probe with visible excitation, has recently been reported.[5] A highly sensitive (K_d <10 pM) carbonic-anhydrase-based zinc sensor that operates by a FRET mechanism is also available.[13]

We envisioned a ratiometric two-fluorophore sensing system in which a zinc-sensitive component was linked to a zinc-insensitive reporter in such a manner that the two would separate upon entering the cell. An ester-linked system seemed ideal for this application because carboxylate esterification is a common strategy in preparing cell-permeable, trappable sensors. The lipophilic esterified sensor can passively diffuse across the cell membrane, and once inside the cell the esters can be hydrolyzed by cytoplasmic esterases, regenerating the membrane-impermeant parent carboxylate **3** and compounds **4** and **5**, which are expected to exhibit good intracellular retention.[5,14−17] Scheme 1 illustrates the strategy.

The synthesis of ZP1 species containing carboxylate functionalities on the bottom ring has been reported elsewhere.[14,15] ZP1 is a fluorescein-based Zn^{2+} sensor that is cell-permeable without prior modification;[16,17] however, fluorescein-based compounds are typically membrane-impermeable owing to the predominance of a charged tautomer in aqueous solutions at neutral pH. Such fluorescein species are permeabilized by protecting the phenolic hydroxyl groups as hydrolytically labile acetates,[18] trapping the fluorescein moiety in the cell-permeable lactone form.[19] Esterification of carboxylates with alkyl or functionalized alkyl groups is widely used for sensors in which the carboxylate is an integral part of the analyte-binding system or is introduced to increase solubility. Acetoxymethyl esters are particularly susceptible to hydrolysis,[19,20] but ethyl esters[9,21,22] are also commonly used, implying that simple alkyl esters are acceptable substrates for cytoplasmic esterases.

Coumazin-1 and -2 (CZ1, **1**; CZ2, **2**) are ZP1 analogues containing coumarin 343 (**3**) as the reporter fluorophore bound via a hydrolyzable alkyl-amidoester or diester linker. Permeation of **1** or **2** into the cell and subsequent cleavage by intracellular esterases thus regenerates the parent fluorophores **3** and **4** or **5**, enabling two-fluorophore ratiometric sensing of Zn^{2+}, as shown in Scheme 1. We report here the synthesis and physical characterization of these molecules as well as biological applications. A preliminary communication describing CZ1 has appeared previously.[14]

Experimental Section

Materials and Methods. Reagents were purchased from Aldrich and used without further purification except for coumarin 343, which was recrystallized from MeOH and CH_2Cl_2 before use. The pyridinium salt of 3′,6′-diacetyl-2′,7′-dichloro-6-carboxyfluorescein (**6**) was prepared as described.[15] A porcine liver esterase (PLE) suspension was purchased from Sigma and used as supplied. SDS-PAGE gel analysis indicated the esterase solution to be a mixture of two major protein components, which we take as a crude estimate of what might be present in cells. The Michaelis−Menten constants reflect average values from PLE treatment. Acetonitrile and dichloromethane were obtained from a dry-still solvent dispensation system. Fluorescence spectra were acquired on a Hitachi F-3010 or a Photon Technology International (Lawrenceville, NJ) Quanta Master 4L-format scanning fluorimeter. The latter was equipped

(13) Thompson, R. B.; Cramer, M. L.; Bozym, R.; Fierke, C. A. *J. Biomed. Opt.* **2002**, *7*, 555−560.
(14) Woodroofe, C. C.; Lippard, S. J. *J. Am. Chem. Soc.* **2003**, *125*, 11458−11459.
(15) Woodroofe, C. C.; Masalha, R.; Barnes, K. R.; Frederickson, C. J.; Lippard, S. J. *Chem. Biol.* **2004**, *11*, 1659−1666.
(16) Walkup, G. K.; Burdette, S. C.; Lippard, S. J.; Tsien, R. Y. *J. Am. Chem Soc.* **2000**, *122*, 5644−5645.
(17) Burdette, S. C.; Walkup, G. K.; Spingler, B.; Tsien, R. Y.; Lippard, S. J. *J. Am. Chem. Soc.* **2001**, *123*, 7831−7841.
(18) Adamczyk, M.; Chan, C. M.; Fino, J. R.; Mattingly, P. G. *J. Org. Chem.* **2000**, *65*, 596−601.
(19) Haugland, R. P. *Handbook of Fluorescent Probes and Research Products, Ninth Edition*; Molecular Probes, Inc.: Eugene, OR, 2002.
(20) Tsien, R. Y.; Pozzan, T.; Rink, T. J. *J. Cell Biol.* **1982**, *94*, 325−334.
(21) Zalewski, P. D.; Millard, S. H.; Forbes, I. J.; Kapaniris, O.; Slavotinek, A.; Betts, W. H.; Ward, A. D.; Lincoln, S. F.; Mahadevan, I. *J. Histochem. Cytochem.* **1994**, *42*, 877−884.
(22) Nasir, M. S.; Fahrni, C. J.; Suhy, D. A.; Kolodsick, K. J.; Singer, C. P.; O'Halloran, T. V. *J. Biol. Inorg. Chem.* **1999**, *4*, 775−783.

with an LPS-220B 75-W xenon lamp and power supply, an A-1010B lamp housing with integrated igniter, a switchable 814 photon-counting/analog PMT detector, and an MD-5020 motor driver. A Perkin-Elmer AAnalyst-300 atomic absorption spectrophotometer (AAS) with a Perkin-Elmer HGA-800 Graphic Furnace (GF-AAS) was used for atomic absorption (AA) spectroscopy measurements. UV−visible absorption spectra were recorded on a Cary 1E UV−visible spectrophotometer at 25 °C. Both were analyzed by using Kaleidagraph 3.0 for Windows. ^{1}H and ^{13}C NMR spectra were acquired on a Varian 300 or 500 MHz or a Bruker 400 MHz spectrometer. High-resolution mass spectra were recorded on an FTMS electrospray apparatus by personnel at the MIT Department of Chemistry Instrumentation Facility. LCMS analysis was performed on an Agilent Technologies 1100 Series LCMS with a Zorbax Extend C-18 column using a linear gradient of 100% A (95:5 H_2O:MeCN, 0.05% HCO_2H) to 100% B (95:5 MeCN:H_2O; 0.05% HCO_2H) over 30 min at a flow rate of 0.250 mL/min. Detector wavelengths were set at 240 and 500 nm, and the MS detector was set to positive ion mode scanning the range m/z = 100−2000.

Synthetic Procedures. (a) *N*-(2-Hydroxyethyl)-3′,6′-diacetyl-2′,7′-dichlorofluorescein-6-amide (9). The pyridinium salt of 3′,6′-diacetyl-2′,7′-dichloro-6-carboxyfluorescein (**6**, 1.22 g, 2 mmol) was dissolved in dry CH_2Cl_2 containing 400 μL of DMF and stirred in a dry ice-acetone bath. Oxalyl chloride (1.5 mL, 2 M solution in CH_2Cl_2) was diluted with 25 mL of dry CH_2Cl_2 and added dropwise over 30 min. The reaction was stirred for an additional 30 min and then concentrated under reduced pressure. The resulting residue was dissolved in CH_2Cl_2, $NaHCO_3$ (336 mg, 4 mmol) was added, and the suspension was stirred at −78 °C as a solution of ethanolamine (390 μL, 409 mg, 6.6 mmol) in 15 mL of CH_2Cl_2 was added dropwise. The reaction was stirred overnight, at which time 40 mL of H_2O was added and the layers were separated. The aqueous layer was washed with 2 × 40 mL CH_2Cl_2; the combined organic layers were washed with saturated NaCl solution, dried over $MgSO_4$, and evaporated. The resulting residue was purified by flash chromatography on silica gel eluting with 98:2 → 96:4 $CHCl_3$:MeOH to give 450 mg (42%) of **9** as a colorless solid. ^{1}H NMR ($CDCl_3$): δ 8.10 (s, 2 H); 7.56 (s, 1 H); 7.11 (s, 2 H); 7.08 (t, 1 H); 6.84 (s, 1 H); 3.70 (t, 2 H); 3.49 (m, 2 H); 2.37 (s, 6 H). ^{13}C NMR ($CDCl_3$): δ 168.40, 167.79, 166.32, 152.42, 149.72, 148.82, 141.52, 130.37, 129.15, 128.02, 126.27, 123.09, 122.53, 117.09, 113.04, 80.67, 61.79, 43.03, 20.82. mp 159−162 °C. HRMS (M + H): calcd for $C_{27}H_{20}Cl_2NO_9$: 572.0515; found 572.0529.

(b) Mitsunobu Reaction of *N*-(2-Hydroxyethyl)-3′,6′-diacetyl-2′,7′-dichloro-fluorescein-6-amide. *N*-(2-Hydroxyethyl)-3′,6′-diacetyl-2′,7′-dichlorofluorescein-6-amide (**9**, 55 mg, 0.1 mmol) was combined with coumarin 343 (29 mg, 0.1 mmol), triphenylphosphine (30 mg, 0.11 mmol), and DIAD (21 μL, 0.1 mmol) in dry CH_2Cl_2 and stirred 45 min at RT. The reaction was concentrated in vacuo, the residue was dissolved in minimal CH_2Cl_2, and Et_2O was added. The resulting orange crystalline solid was filtered off and one-half of the filtrate was loaded onto a preparative scale TLC plate. Compound **10** was isolated as the major product (17 mg, corresponds to 64% overall yield). ^{1}H NMR ($CDCl_3$): δ 8.28 (d, 1 H); 8.12 (d, 1 H); 7.76 (s, 1 H); 7.16 (s, 2 H); 6.87 (s, 2 H); 4.47 (t, 2 H); 4.08 (t, 2 H); 2.38 (s, 6 H). HRMS (M + Na): calcd for $C_{27}H_{17}Cl_2NO_8Na$: 576.0229; found 576.0216.

(c) Coumarin 343 4-Hydroxybutyl Ester (11). Coumarin 343 (**3**, 285 mg, 1 mmol) was combined with 4-benzyloxy-1-butanol (190 μL, 1.03 mmol), triphenylphosphine (280 mg, 1.07 mmol), and DIAD (210 μL, 1.01 mmol) in 20 mL of dry CH_2Cl_2. The reaction was stirred at RT for 90 min and then quenched with 20 mL of MeOH. Pd/C was added and the suspension was stirred under a H_2 atmosphere for 2 h, then filtered through Celite, and concentrated in vacuo. The viscous residue was purified by flash chromatography on silica gel eluting with 93:7 $CHCl_3$:MeOH and then crystallized from $CHCl_3$ layered with Et_2O. Filtration gave 277 mg of **11** (78% yield). ^{1}H NMR ($CDCl_3$): δ 8.36 (s, 1 H); 6.95 (s, 1 H); 4.35 (t, 2 H); 3.74 (t, 2 H); 3.34 (m, 4 H); 2.87 (t, 2 H); 2.77 (t, 2 H); 1.98 (m, 4 H); 1.75 (m, 4 H). ^{13}C NMR ($CDCl_3$): δ 165.11, 159.20, 153.64, 149.76, 148.82, 127.19, 119.47, 107.76, 107.18, 105.82, 65.39, 62.06, 50.43, 50.04, 29.91, 27.57, 25.00, 21.27, 20.29, 20.18. mp 135−137 °C. HRMS (M + Na) calcd for $C_{20}H_{23}NO_5Na$: 380.1474; found 380.1463.

(d) Coumarin 343 4-(6-Carboxy-3′,6′-diacetyl-2′,7′-dichloro-fluorescein)butyl Ester (12). Coumarin 343 4-hydroxybutyl ester (**11**, 268 mg, 0.75 mmol) was combined with 6-carboxy-2′,7′-dichlorofluorescein-3′,6′-diacetate pyridinium salt (479 mg, 0.78 mmol), triphenylphosphine (206 mg, 0.78 mmol), and DIAD (158 μL) in 30 mL of dry CH_2Cl_2 at RT and stirred overnight. More DIAD (79 μL) was then added. After 24 h the reaction was concentrated in vacuo and the desired product was isolated by flash chromatography on silica gel eluting with 98:2 → 90:10 $CHCl_3$:MeOH, followed by trituration with MeOH to give 185 mg (28%) of **12**. ^{1}H NMR ($CDCl_3$): δ 8.38 (d, 1 H); 8.31 (s, 1 H); 8.14 (d, 1 H); 7.84 (s, 1 H); 7.18 (s, 2 H); 6.94 (s, 1 H); 6.85 (s, 2 H); 4.42 (t, 2 H); 4.35 (t, 2 H); 3.34 (m, 4 H); 2.88 (t, 2 H); 2.76 (t, 2 H); 2.38 (s, 6 H); 1.9−2.0 (m, 8 H). ^{13}C NMR ($CDCl_3$): δ 168.08, 167.78, 164.88, 158.81, 153.70, 152.12, 149.86, 149.49, 148.85, 148.78, 137.57, 132.16, 129.17, 129.06, 127.18, 126.02, 125.39, 123.02, 119.37, 117.09, 113.11, 107.71, 107.38, 105.93, 80.95, 65.03, 64.44, 50.46, 50.07, 26.61, 24.60, 24.56, 21.33, 20.83, 20.35, 20.25. mp dec > 159 °C. HRMS (M + Na): calcd for $C_{45}H_{35}Cl_2NO_{13}Na$: 890.1383; found 890.1414.

(e) Coumazin-2 (2). Dipicolylamine (128 mg, 0.64 mmol) and paraformaldehyde (40 mg, 1.32 mmol) were combined in 10 mL of dry MeCN and heated to reflux for 45 min. A portion of **12** (87 mg, 0.1 mmol) was suspended in 5 mL of MeCN and added to the refluxing solution, followed by 5 mL of H_2O. The reaction was heated at reflux for 24 h, at which time it was cooled to RT, concentrated in vacuo, acidified with 5 drops of glacial acetic acid, and stored at 4 °C overnight. The resulting red precipitate was filtered to afford 87 mg (72%) of **2**. ^{1}H NMR ($CDCl_3$): δ 8.60 (d, 4 H); 8.38 (d, 2 H); 8.33 (s, 1 H); 8.10 (d, 1 H); 7.85 (s, 1 H); 7.67 (td, 4 H); 7.36 (d, 4 H); 7.20 (m, 4 H); 6.97 (s, 1 H); 6.60 (s, 2 H); 4.40 (t, 2 H); 4.32 (t, 2 H); 4.20 (s, 4 H); 4.01 (m, 8 H); 3.34 (m, 4 H); 2.86 (t, 2 H); 2.75 (t, 2 H); 1.80−1.98 (m, 12 H). mp dec > 151 °C. HRMS (M + H): calcd for $C_{67}H_{58}Cl_2N_7O_{11}$: 1206.3571; found 1206.3564.

(f) 6-Carboxy-2′,7′-dichlorofluorescein-3′,6′-diacetatesuccinimidyl Ester (15). The pyridinium salt of 6-carboxy-2′,7′-dichlorofluorescein-3′,6′-diacetate (**6**, 945 mg, 1.5 mmol) was combined with 1-[3-(dimethylamino)propyl]-3-ethylcarbodiimide hydrochloride (EDC) (300 mg, 1.56 mmol) and *N*-hydroxysuccinimide (200 mg, 1.74 mmol) in 10 mL of 1:1 ethyl acetate:DMF and stirred at RT for 6 h. Brine (75 mL) and CH_2Cl_2 (50 mL) were added, and the layers were separated. The aqueous layer was extracted with 2 × 50 mL CH_2Cl_2; the combined organics were washed with 2 × 50 mL of 0.1 N HCl and 1 × 50 mL of brine, dried over $MgSO_4$, and evaporated. The resulting residue was purified by flash chromatography on silica gel eluting with 99:1 $CHCl_3$:MeOH to give 647 mg (0.48 mmol, 69%) of **15** as a glassy foam. ^{1}H NMR ($CDCl_3$): δ 8.44 (d, 1 H); 8.22 (d, 1 H); 7.93 (s, 1 H); 7.19 (s, 2 H); 6.84 (s, 2 H); 2.90 (dd, 4 H); 2.37 (s, 6 H). ^{13}C NMR ($CDCl_3$): δ 168.90, 167.90, 167.00, 162.61, 160.43, 152.17, 149.62, 148.88,

132.72, 132.07, 130.66, 128.89, 126.30, 123.07, 116.36, 113.06, 80.84, 25.61, 20.67. mp 84−86 °C. HRMS (M + H): calcd for $C_{29}H_{18}Cl_2NO_{11}$: 626.0257; found 626.0220.

(g) *N*-(4-Hydroxybutyl)-2′,7′-dichlorofluorescein-6-amide (16). 6-Carboxy-2′,7′-dichlorofluorescein-3′,6′-diacetate succinimidyl ester (**15**, 312 mg, 0.5 mmol) was dissolved in 1:1 CH_2Cl_2:MeOH and stirred at RT with 4-aminobutanol (230 μL, 222 mg, 2.5 mmol) overnight. The resulting red solution was concentrated on the rotary evaporator, taken up in 10 mL of H_2O, acidified with concentrated HCl, and filtered to afford an orange solid, which was dried overnight to give 235 mg of **16** (91% yield). ^{1}H NMR (MeOH-d_4): δ 8.15 (s, 2 H); 7.62 (s, 1 H); 6.85 (s, 2 H); 6.68 (s, 2 H); 3.57 (t, 2 H); 3.35 (m, 2 H); 1.50−1.65 (m, 4 H). mp 179−180 °C (dec). HRMS (M − H): calcd for $C_{25}H_{18}Cl_2NO_7$: 514.0460; found 514.0474.

(h) ZP1(6-CONH(CH$_2$)$_4$OH) (4). Dipicolylamine (256 mg, 1.3 mmol) was combined with paraformaldehyde (36 mg, 2.6 mmol) in 10 mL of dry MeCN and heated to reflux for 45 min. *N*-(4-Hydroxybutyl)-2′,7′-dichlorofluorescein-6-amide (103 mg, 0.2 mmol) was suspended in 15 mL of 1:1 MeCN:H_2O and added to the reaction, and reflux was continued for 24 h. The reaction was cooled to RT, acidified with 0.5 mL of glacial acetic acid, and concentrated under reduced pressure. The residue was diluted with MeOH and H_2O and stored at 4 °C overnight. Filtration afforded the desired product (19 mg, 10%). ^{1}H NMR (MeOH-d_4): δ 8.53 (d, 4 H); 8.12 (s, 2 H); 7.63 (s, 1 H); 7.48 (d, 4 H); 7.30 (m, 4 H); 7.26 (t, 4 H); 6.67 (s, 2 H); 4.34 (s, 4 H); 4.18 (m, 8 H); 3.52 (t, 2 H); 3.37 (t, 2 H); 1.52−1.68 (m, 4 H). mp 157−159 °C (dec). HRMS (M + H): calcd for $C_{51}H_{46}Cl_2N_7O_7$: 938.2836; found 938.2843.

Spectroscopic Measurements. All glassware was washed sequentially with 20% HNO_3, deionized water, and ethanol before use. Purified water (resistivity 18.2 MΩ) was obtained from a Millipore Milli-Q water purification system. Fluorophore stock solutions in DMSO were made up to concentrations of 1 mM and kept at 4 °C in 100−500 μL aliquots. Portions were thawed and diluted to the required concentrations immediately prior to each experiment. Fluorescence and absorption data were measured in HEPES buffer (50 mM, pH 7.5, KCl 100 mM) except for fluorometric pK_a titrations, which were performed in 100 mM KCl, pH 12.5, and for the fluorescein standard in quantum yield measurements, which was measured in 0.1 N NaOH. The HEPES buffer, prepared with Millipore water, contains 20 ± 2 mg/L (0.3 ± 0.03 μM) of zinc as determined by flameless atomic absorption (AA) spectroscopy. Solutions were stored in clean, dry propylene containers and were filtered (0.25 μm) before data acquisition. Fluorescence spectra were recorded from 425 to 650 nm. Extinction coefficients, quantum yields, fluorescence-dependent pK_a values, and dissociation constants were measured as previously described.[14] All measurements were performed in triplicate.

(a) Zn^{2+} Response of Esterase-Treated CZ Dyes. A 10 mL portion of a 4 μM solution of CZ1 in pH 7.5 HEPES buffer was incubated with a 10 μL aliquot of PLE (10 mg/mL in 3.2 M $(NH_4)_2SO_4$) at RT for 12 h. A 2 mL aliquot was withdrawn and the fluorescence spectrum from 425 to 650 nm was acquired with excitation first at 445 nm and then at 505 nm. A 4 μL aliquot of 10 mM $ZnCl_2$ was added and the fluorescence spectra were recorded as before. The procedure was repeated for CZ2 with incubation times varying from 1 to 6 h.

(b) Michaelis−Menten Kinetics of Esterase Hydrolysis of CZ2. A 5 μL aliquot of PLE was added to a fluorescence cuvette containing 2 mL of pH 7.5 HEPES buffer and various concentrations (0.5 nM − 25 μM) of CZ2. The cuvette was shaken vigorously and the emission intensity at 488 nm (excitation 445 nm) was monitored for 5 min at 25 °C. The rate of increase in emission intensity between 100 and 200 s was determined and converted to μmol/min of coumarin 343 produced using a standard curve. The rate of increase in concentration of coumarin 343 was plotted as a function of substrate concentration and fit by using a Michaelis−Menten model.

(c) LCMS Determination of CZ1 and CZ2 Ester Hydrolysis Products. A 10 μM solution of CZ1 (20 μL of a 1 mM DMSO stock solution of CZ1 and 5 μL PLE suspension in 2 mL HEPES buffer (50 mM, pH 7.5)) was incubated 19 h at 22 °C in a polystyrene tube covered with aluminum foil, filtered, and analyzed by LCMS. The major peaks observed were at 10.8 min (no assignable mass), 13.0 min (m/z = 469.9), and 18.4 min (m/z = 593.1). A 10 μM solution of CZ2 was similarly prepared and incubated for 1 h before LCMS analysis. The major peaks observed were at 14.8 min (m/z = 939.2) and 18.1 min (m/z = 593.1). Retention times were determined for 10 μM standard solutions of expected metabolites for comparison and were as follows: **3** 18.5 min (m/z = 593.1; calcd for 2M + Na = 593.2); **4** 12.9 min (m/z = 469.2; calcd for (M + 2H)/2 = 469.2); **11** 17.2 min (m/z = 380.3; calcd for M + Na = 380.2).

(d) Absorption Spectroscopy of PLE-Treated CZ1 and CZ2. A 20 μL aliquot of 1 mM CZ1 stock solution (DMSO) was added to 2 mL of HEPES buffer. A 10 μL aliquot of PLE suspension was added, and the absorbance spectrum was acquired periodically over 6 h. The procedure was repeated for CZ2.

Imaging. HeLa cells were grown at 37 °C under a 5% CO_2 atmosphere in Dulbecco's modified Eagle's medium (DMEM, Gibco/BRL) supplemented with 10% fetal bovine serum, 1x penicillin/streptomycin, and 2 mM L-glutamine. Coumazin-1 and Coumazin-2 were stable in EMEM and DMEM over 4 h at 37 °C under conditions used for cell studies, as monitored by fluorescence at both excitation wavelengths (445 or 505 nm). Cells were plated 24 h before study into 2 mL imaging dishes. Cells were approximately 50% confluent at the time of study. A 20 μL aliquot of dye (1 mM DMSO) was added to each 2 mL dish, and the cells were incubated for 4 h at 37 °C, at which point the medium was aspirated and the cells were washed twice with phosphate-buffered saline solution (PBS), resuspended in dye-free EMEM (Mediatech), and examined on a Zeiss Axiovert 200M inverted epifluorescence microscope with a 40× oil immersion, a mercury lamp light source, and differential interference contrast (DIC), operated by OpenLab software (Improvision, Lexington, MA). Samples were maintained at 37 °C over the course of the imaging experiment. The amount of zinc in the cell growth medium was 20 ± 2 μg/L (0.3 ± 0.03 μM) and 60 ± 2 μg/L (0.9 ± 0.03 μM) for DMEM and EMEM, respectively, as determined by flameless AA spectroscopy. Images were collected at 30 s intervals for 30 min during the course of the experiment, as a 10 μL aliquot of a solution containing 1 μM $ZnCl_2$ and 9 μM sodium pyrithione was added. The fluorescence response reached a maximum at about 10−15 min after addition of $ZnCl_2$, at which time a 10 μL aliquot of 10 μM TPEN was added. At each time point, four images were collected in rapid succession: a DIC image (775DF50 emission) and three fluorescence images using a CFP filter (420DF20 excitation, 450DRLP dichroic, 475DF40 emission), a FRET filter (420DF20 excitation, 450DRLP dichroic, 530DR30 emission), and a YFP filter (495DF10 excitation, 515DRLP dichroic, 530DF30 emission). Fluorescence images were background-corrected. Acquisition times were in the range of 100−250 ms. A control experiment in which a 10 μL aliquot of 10 μM TPEN was added to the imaging dish without prior addition of exogenous $ZnCl_2$ was performed using a similar protocol.

Scheme 2. Synthesis of CZ Dyes

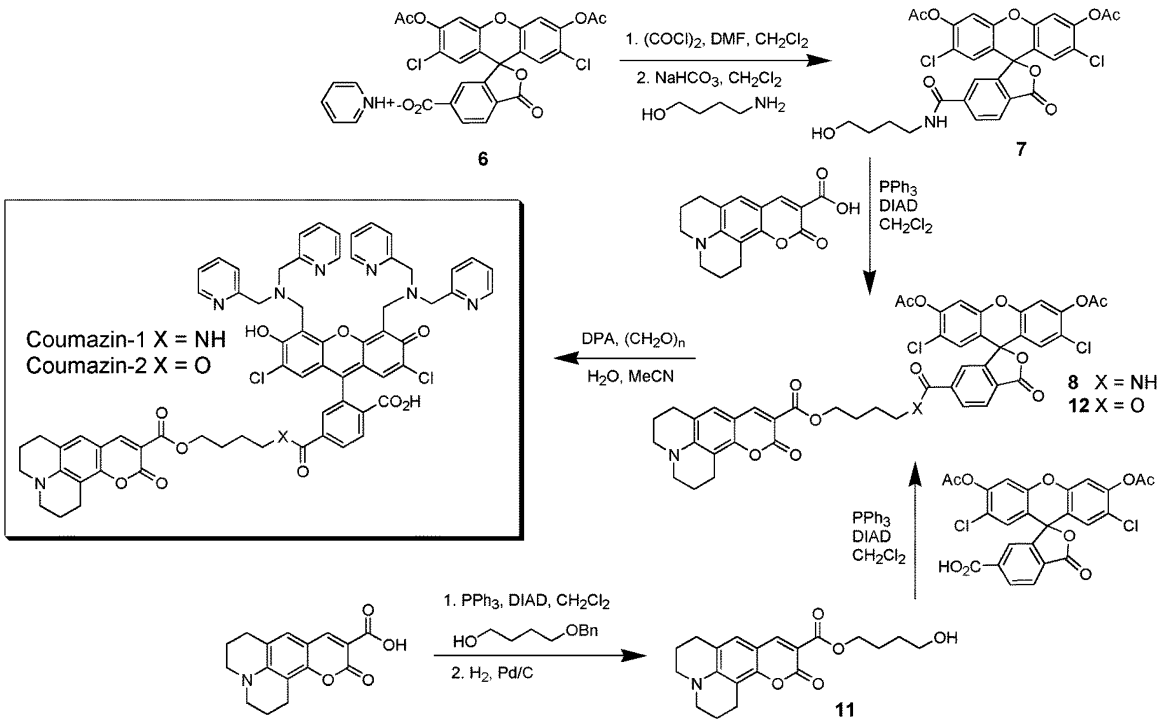

Scheme 3. Intramolecular Cyclization under Mitsunobu Conditions

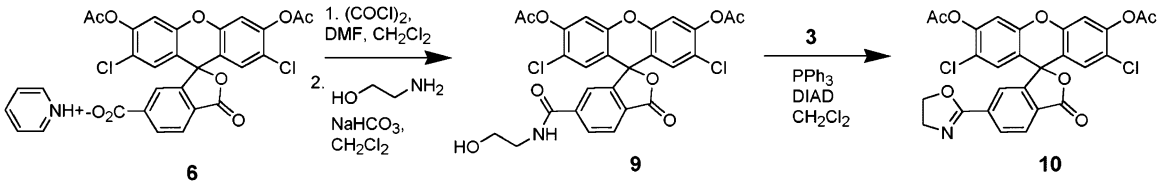

Results and Discussion

Synthesis. The compounds Coumazin-1 and -2 were synthesized as shown in Scheme 2. The choice of an *n*-butyl linker in the synthesis of CZ1[14] was not arbitrary. Our initial approach involved the hydroxyethylamide **9**; however, the Mitsunobu condensation conditions gave primarily the intramolecular cyclization product **10**, as shown in Scheme 3. Oxazole formation of β-hydroxyethyl amides under Mitsunobu conditions is well precedented in the literature,[23−25] notably in syntheses of paclitaxel and related compounds. Similar problems were encountered with a propyl linker (data not shown). The butyl linker would form a thermodynamically unfavorable seven-membered ring as the product of such an intramolecular condensation, allowing the desired intermolecular reaction to dominate.

The approach to Coumazin-2 (CZ2) was slightly different. Mitsunobu condensation of coumarin 343 with 4-benzyloxyl-1-butanol followed by hydrogenation furnished the coumarin hydroxybutyl ester **11** in 78% yield over two steps. Removal of the diisopropyl hydrazidodicarboxylate byproduct from the intermediate benzyl ether was extremely difficult and reduced the overall yield; hence, the most expedient route was to carry the undesired byproduct through and remove it from the deprotected **11** by crystallization. A second Mitsunobu reaction of **11** with the diacetyldichlorofluorescein carboxylate **6** was sluggish, proceeding only to 28% conversion. The reaction yield was not improved by using the free acid of the fluorescein moiety rather than the pyridinium salt. The resulting diester-linked fluorescein-coumarin compound **12** was subjected to standard Mannich conditions and furnished the desired coumpound CZ2 (**2**) in 72% yield.

The expected ZP hydrolysis product **4** of CZ1 was synthesized as shown in Scheme 4. Determination of the photophysical and thermodynamic properties of **4** confirmed that the extension of the alkyl chain by two methylene units does not noticeably alter the fluorescence properties or Zn^{2+} response of **4** as compared with the previously reported analogue **13**. Oxalyl chloride activation was employed in the synthesis of **13**; however, this reaction was sensitive to a variety of experimental factors and the extent of conversion to the acid chloride was somewhat variable, leading to mixtures that included deprotected starting material. Alternative methods of activation were therefore sought. EDC-mediated coupling of **6** to *N*-hydroxysuccinimide proceeded in reasonable yield to give the succinimidyl ester **15**, an activated intermediate that can be purified by column chromatography. Subsequent reaction with a 3-fold or greater

(23) Hamamoto, H.; Mamedov, V. A.; Kitamoto, M.; Hayashi, N.; Tsuboi, S. *Tetrahedron: Asymmetry* **2000**, *11*, 4485−4497.
(24) Cevallos, A.; Rios, R.; Moyano, A.; Pericàs, M. A.; Riera, A. *Tetrahedron: Asymmetry* **2000**, *11*, 4407−4416.
(25) Mandai, T.; Kuroda, A.; Okumoto, H.; Nakanishi, K.; Mikuni, K.; Hara, K.; Hara, K. *Tetrahedron Lett.* **1999**, *41*, 243−246.

Scheme 4. Synthesis of Putative ZP1 Metabolites

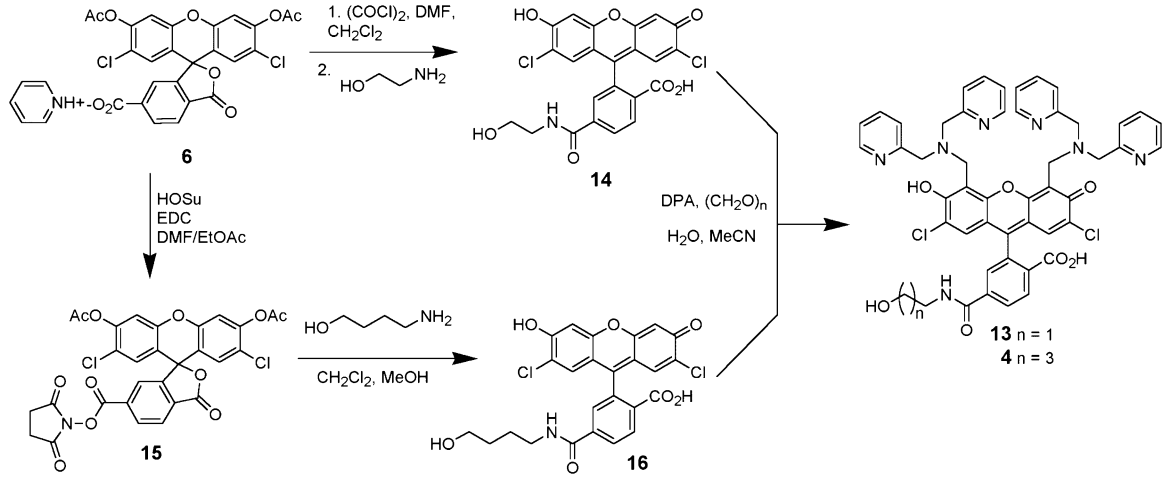

Scheme 5. Possible Esterase Digestion Products of CZ2

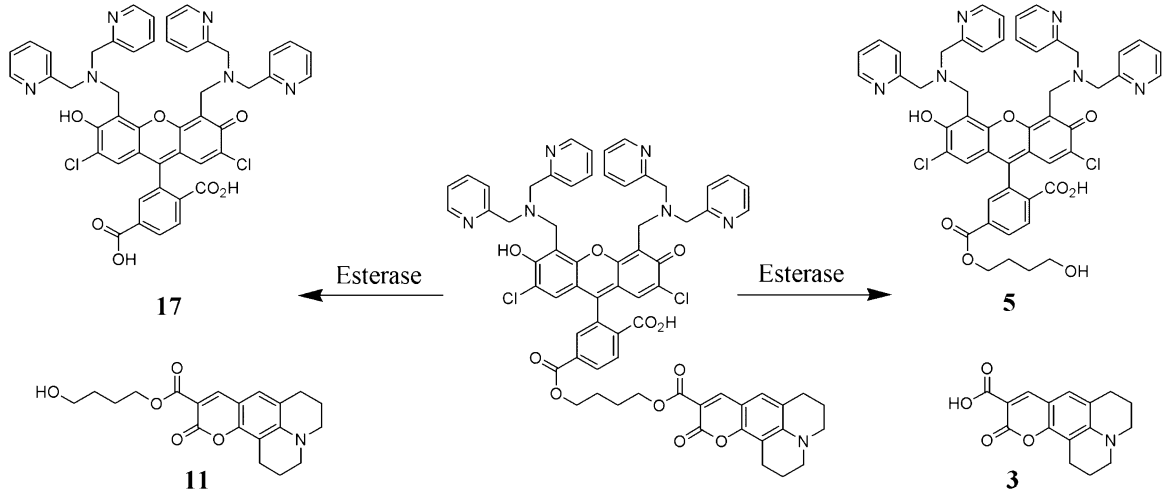

excess of amine in mixed CH_2Cl_2/MeOH yielded the deprotected fluoresceinamide **16**, which can be isolated by simple precipitation after removal of organic solvents, providing a straightforward and practical route to simple fluoresceinamides. Subsequent Mannich reaction of **14** furnished the desired amide-substituted ZP1 adduct **4**. Extinction coefficients and quantum yields for **4** with and without Zn^{2+} were measured, and the dissociation constants and fluorescence response of **4** to Zn^{2+} are essentially identical to those of the previously reported **13**.[14] CZ2 contains two possible sites for ester hydrolysis. Esterase digestion can therefore produce ZP1 hydroxybutyl ester **5** or ZP1(6-CO_2H) (**17**), as shown in Scheme 5. The Zn^{2+}-sensing properties of ester- or acid-functionalized ZP1 carboxylates have been described elswhere.[13] Measured constants for putative CZ fragments or analogues thereof are listed in Table 1. All of these ZP1-like hydrolysis products may be expected to function effectively as Zn^{2+} sensors.

Table 1. Photochemical Properties of CZ Dyes and Their Expected Cleavage Fragments

	ϵ ($M^{-1}\,cm^{-1}$)	λ_{max} (nm) absorbance	Φ_{ZP1}	$\Phi_{Coumarin}$	K_d (nM)	pK_a
4	62000	519	0.22		0.25	–
4 + Zn^{2+}	65000	509	0.69			
13	71100	518	0.21		0.20	8.43
13 + Zn^{2+}	78600	508	0.67			
17[a]	76000	516	0.21		0.16	7.12
17 + Zn^{2+}	81000	506	0.63			
ZP1-6-CO_2Et[b]	61000	519	0.13		0.37	7.00
+ Zn^{2+}	72000	509	0.67			
CZ1[a]	37200	451,	0.02	0.01	0.25	
	38600	526				
CZ1 + Zn^{2+}	41000	449,	0.04	0.01		
	38100	518				
CZ2	26000	450,	0.02	0.01		
	22400	526				
CZ2 + Zn^{2+}	26567	448,	0.04	0.01		
	24333	521				

[a] Data reproduced from ref 14 for comparison purposes. [b] Data reproduced from ref 15.

Photophysics and Thermodynamics. The photophysical properties of CZ1 and CZ2 have been examined, and relevant data are listed in Table 1. Both coumazin compounds fluoresce extremely weakly prior to esterase processing, regardless of the fluorophore excited. Whereas a Förster resonance energy transfer (FRET) mechanism might account for quenching of the putative donor, such a process would require a concomitant increase in the fluorescence emission of the putative acceptor, which is not observed. ZP1 fluorescence in both cases is similarly quenched, implying that the Förster interaction is not the major mechanism of

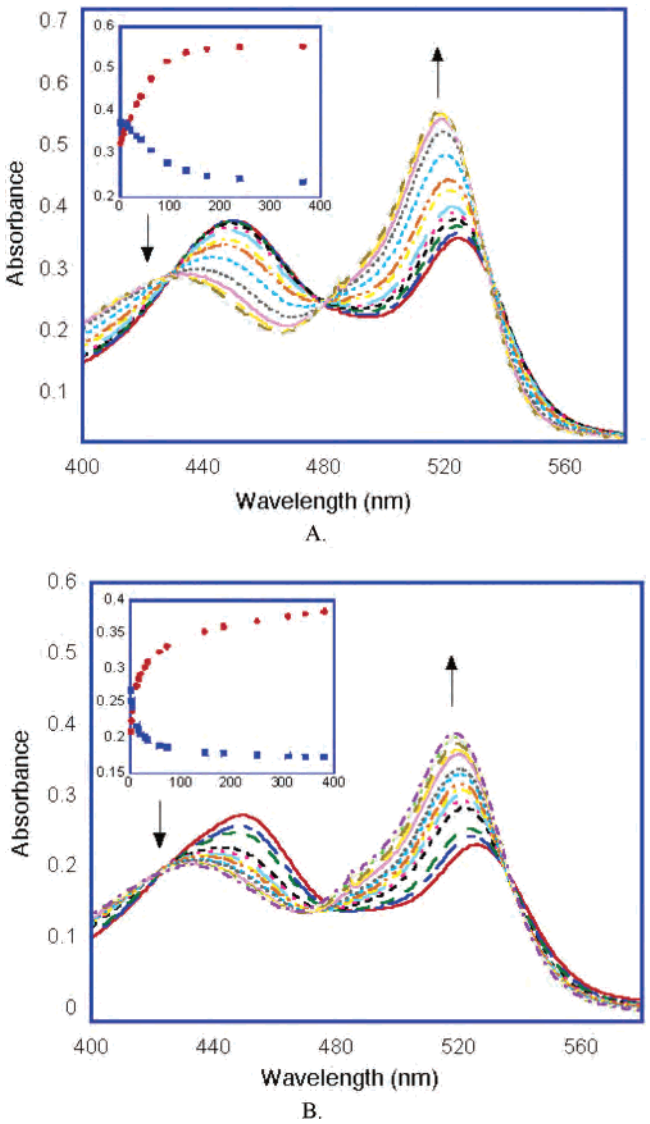

Figure 1. Time-dependent changes in absorption spectra for CZ1 over 6 h (A) and CZ2 over 3 h (B) upon treatment with porcine liver esterase. Insets: changes in absorption at 519 nm (red circles) and 450 nm (blue squares) as a function of time (min).

quenching.[26] In addition, the extinction coefficients of CZ1 and CZ2 are significantly reduced in comparison to their ZP counterparts (Table 1). Treatment of either CZ1 or CZ2 with porcine liver esterase (PLE) effects an increase in intensity of nearly 100% and a blue shift from 526 to 519 nm in the absorption band corresponding to the ZP1 absorbance (Figure 1). The coumarin absorption band similarly undergoes a blue shift from 450 to 435 nm, but the intensity of the band decreases by approximately 40%. The lack of a perfectly clean isosbestic point at 480 nm for CZ2 compared to CZ1 may indicate multiple reactions, possibly because of the potential for hydrolysis at two sites. This extreme change signals a strong interaction between fluorophores and is further evidence that the Förster mechanism, a weak interaction that requires little to no alteration in the absorption

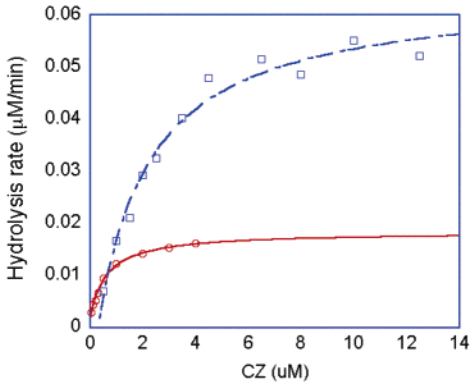

Figure 2. Michaelis−Menten fit of the CZ esterase hydrolysis rate. CZ1 (red circles) was treated with 75 nM PLE, and CZ2 (blue squares) was treated with 37.5 nM PLE. For both compounds, measurements were made at 25 °C in HEPES buffer (pH 7.5). Hydrolysis rate was assumed to be the rate of production of coumarin 343, determined by using a standard curve.

Table 2. Michaelis−Menten Constants for CZ Dyes

	k_{cat} (min^{-1})	k_{cat}/K_M ($\mu M^{-1}\,min^{-1}$)
CZ1	0.017	0.027
CZ2	0.211	0.128

spectrum, is probably not operative.[27] Other reports of such extreme quenching in the case of covalently linked FRET-capable fluorophores, combined with significant changes in the absorption spectrum, have been accounted for by exciton theory,[26,28] and such may be the case here. Quantum yields determined over a 0.1−2.0 μM range were identical within experimental error, indicating no contribution of intermolecular quenching to the mechanism.

The kinetics of PLE action on both compounds were assayed fluorimetrically (Figure 2), revealing that, like the changes in the absorption spectrum, the fluorescence increases much more rapidly for CZ2 than for CZ1. Hydrolysis of either ester in CZ2 will afford roughly the same fluorescence increase. Similarly, after the first hydrolysis event for each CZ2 molecule, the second hydrolysis event will show no fluorescence response but may act as a competing substrate. Although the Michaelis−Menten constants (Table 2) measured for CZ2 are valid for comparison of the fluorescence response with values measured for CZ1, the fluorescence response may arise from more than one reaction and the reported values are therefore considered to be only rough approximations. Nonetheless, hydrolysis of CZ2 is clearly much more efficient than hydrolysis of CZ1, with significantly greater pseudo-k_{cat} (12.4-fold) and pseudo-k_{cat}/K_M (4.7-fold) values (Table 2). Such a large effect cannot be explained by the statistical presence of twice as many substrates and was initially attributed to greater activity of PLE on the ZP1 ester compared to the coumarin ester. To examine this possibility, the CZ2 PLE cleavage products were analyzed by LCMS after 1 h of incubation. The major peaks observed appeared with retention times of 14.8 min (m/z (M + H) = 939.2) and 18.1 min (m/z (2M + H +

(26) Packard, B. Z.; Toptygin, D. D.; Komoriya, A.; Brand, L. *Biophys. Chem.* **1997**, *67*, 167−176.
(27) Foerster, T. In *Modern Quantum Chemistry*; Sinanoglu, O., Ed.; Academic Press: New York, 1965; Vol. 3, pp 99−137.
(28) Packard, B. Z.; Toptygin, D. D.; Komoriya, A.; Brand, L. *Proc. Natl. Acad. Sci. U.S.A.* **1996**, *93*, 11640−11645.

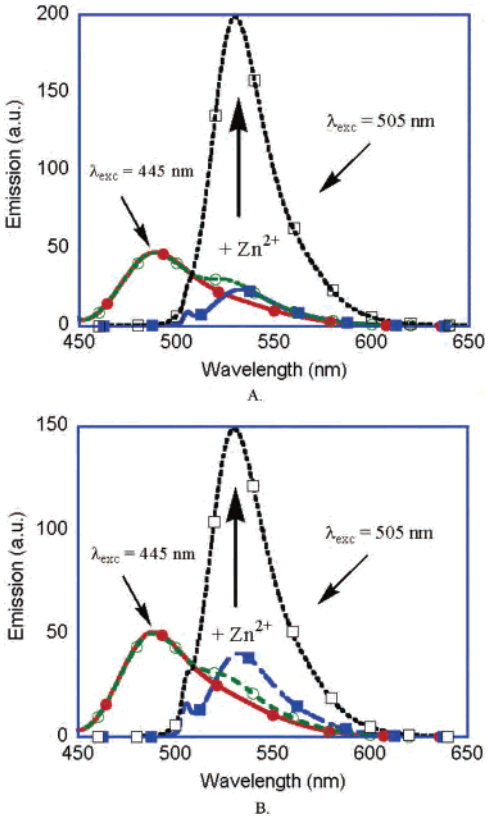

Figure 3. Fluorescence response of esterase-treated CZ1 (A) and CZ2 (B). Aliquots (10 mL) of HEPES buffer containing 2 μM dye were treated with porcine liver esterase for 19 h (CZ1, A) or 4 h (CZ2, B) and emission spectra were recorded with excitation at 445 nm (red solid circles) and 505 nm (blue solid squares). A 10 μM portion of $ZnCl_2$ was added, and emission spectra were again recorded with excitation at 445 nm (green open circles) and 505 nm (black open squares).

Na)/2 = 593.1), corresponding to **5** and **3**, respectively. These products are expected from hydrolysis at the coumarin ester (Scheme 4). Since no peak or signal for **17** could be observed during a standard run, its absence in the CZ2 product mix is not conclusive. However, the lack of detectable amounts of the complementary product **11**, which gives a clear signal at 17.2 min (m/z(M + Na) = 380.3) when run in a control, is strong circumstantial evidence that the coumarin ester is cleaved first with good selectivity. Thus, the increase in rate of hydrolysis appears to stem primarily from enhanced activity of the enzyme on **2** over **1.** LCMS analysis of CZ1 after 19 h exposure to PLE showed products of hydrolysis at the single ester functionality, as expected (**4**, 13.0 min, (M + 2H) = 469.9 and **3**, 18.4 min, (2 M + Na) = 593.1).

The fluorescence responses of esterase-treated CZ1 and CZ2 were also examined. As expected, excitation at 445 nm afforded coumarin fluorescence at 490 nm, and the coumarin emission spectrum was largely unaltered upon addition of excess $ZnCl_2$. Calibration curves of zinc chloride addition to CZ1 and CZ2 reveal a linear response for excitation at 505 nm and none when the excitation wavelength was 445 nm (Figures S1 and S2, Supporting Information). Some ZP1 fluorescence at 535 nm is observed for both compounds and increases significantly after addition of Zn^{2+}. This contribution can be excluded by measuring fluorescence intensity at 488 nm or by instituting a cutoff of 500 nm in measuring

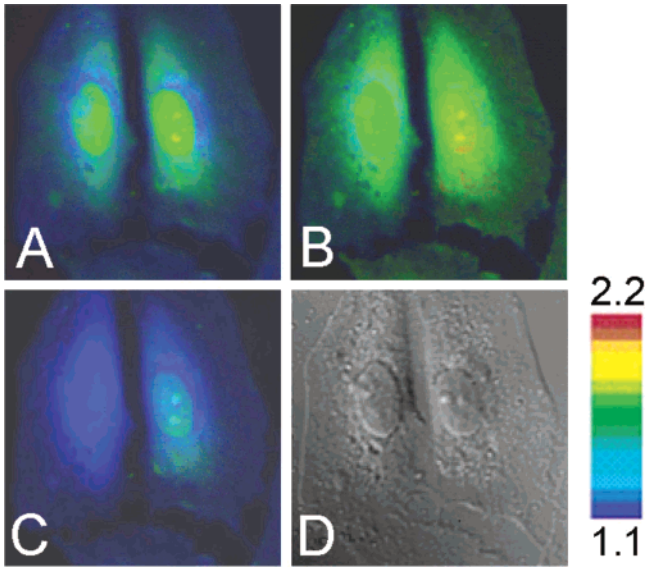

Figure 4. Fluorescence ratio images of HeLa cells treated with CZ2 after addition of $ZnCl_2$ and sodium pyrithione (A, 0 min; B, 8 min), and after subsequent treatment with TPEN (C, 8 min). D: DIC image. Images were acquired at 40× magnification, and the faux-color ratio range was 1.1 (blue)−2.2 (red).

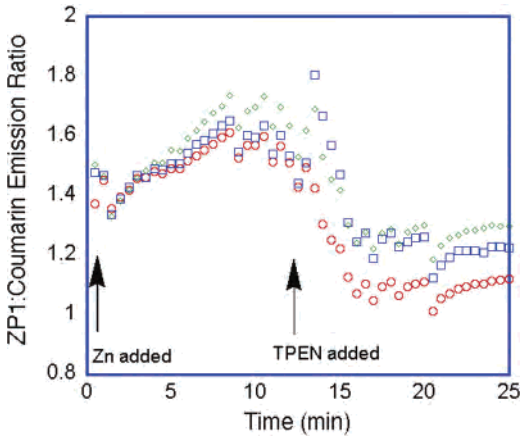

Figure 5. Intensity ratios of ZP1 emission divided by coumarin emission as a function of time. Three separate regions of interest were defined at the start of the experiment and total integrated emission of ZP1 divided by integrated emission of coumarin 343 was measured at 30 s intervals. $ZnCl_2$ (5 μM final concentration) and sodium pyrithione (45 μM) were added at 5 min, and TPEN (50 μM) was added at 17 min.

integrated fluorescence emission area for coumarin. This ZP1 emission band arises from the ability of fluorescein to absorb some photons even when excited at 445 nm. Excitation at 505 nm affords a classic ZP1 emission band, which increases several-fold in response to addition of $ZnCl_2$. Surprisingly, addition of saturating $ZnCl_2$ to esterase-treated CZ2 results in only a 4-fold increase in the ratio of ZP1 integrated emission to coumarin 343 integrated emission compared with the ratio in the absence of Zn^{2+}, whereas an 8-fold increase is observed for CZ1 (Figure 3). The ratio of ZP1:coumarin fluorescence for CZ2 remains relatively constant over several hours.

Biological Imaging. HeLa cells were stained by addition of an aliquot of 1 mM CZ2 in DMSO, to give a final concentration of 10 mM dye in the medium. After incubation for 4 h, the cells were washed and resuspended in dye-free

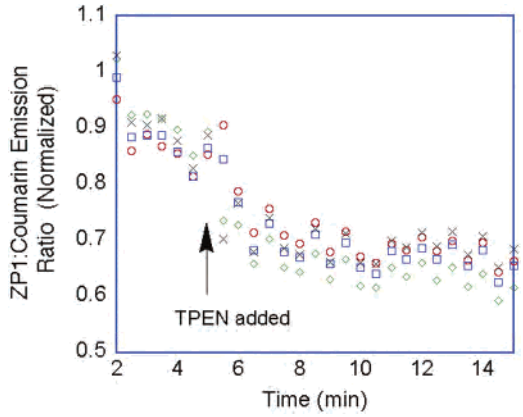

Figure 6. TPEN decreases intensity ratios of ZP1 emission divided by coumarin emission in CZ2-stained HeLa cells without exogenously added zinc. Four separate regions of interest were defined at the start of the experiment and total integrated emission of ZP1 divided by integrated emission of coumarin 343 was measured at 30 s intervals. TPEN (50 μM) was added at 5 min.

medium, and the area immediately surrounding the site of application was imaged (Figure 4). The introduction of $ZnCl_2$-sodium pyrithione resulted in a hyperbolic increase in ZP1 emission over approximately 10 min with no change in coumarin emission (Figure 5). TPEN was added after ZP1 emission had reached an apparent maximum, and the ZP1 emission decreased to slightly lower than initial levels. Coumarin emission was not affected throughout the experiment. The intracellular distribution of the two dyes appears to be reasonably consistent, as assessed by the images after treatment with zinc-pyrithione and after treatment with TPEN. Both dyes are concentrated in the perinuclear area, and relatively good colocalization is observed, based on the Zn^{2+}- and TPEN-treated images (Figure 4B,C). An exception to this general observation is an oval-shaped area in each cell, which displays slightly different intensity ratios compared to its surroundings and probably corresponds to the cell nucleus. This result may arise from different partitioning of the nuclear membrane by the ZP1 and coumarin hydrolysis products, with a corresponding difference in fluorescence ratios. The TPEN-induced decrease in the ZP1:coumarin fluorescence ratio to values below the initial levels probably reflects the presence of some Zn^{2+}-bound dye before exogenous zinc ion and the ionophore are added, because addition of TPEN to CZ2-treated cells without prior addition of Zn^{2+} and pyrithione also decreased the intensity ratio, as shown in Figure 6.

Summary and Conclusions

We describe a new approach to ratiometric sensing of intracellular Zn^{2+} based on the well-known phenomenon of intracellular hydrolysis of esterases. The compounds CZ1 and CZ2 are based on ZP1 sensors linked to the Zn^{2+}-insensitive reporter fluorophore coumarin 343 by an amido-ester or diester moiety. The CZ compounds have very low fluorescence, but upon treatment with porcine liver esterase the ZP1-based Zn^{2+} sensor and reporter fluorophore fluorescence is regenerated. CZ2 is activated more rapidly than CZ1, although the same ester moiety is hydrolyzed first in both cases. CZ2 has been applied to image exogenous Zn^{2+} in HeLa cells and displays an increase in fluorescence ratio upon treatment with Zn^{2+} and an ionophore. The fluorescence ratio decreases below initial levels upon treatment with TPEN, a result in accord with other recent reports.[10]

Acknowledgment. This work was supported by the NIGMS under Grant GM65519. We thank Professor A. Y. Ting and Mr. C.-W. Lin for help in using their epifluorescence microscope. HeLa cells were provided by Mrs. K. R. Barnes and Ms. C. Saouma.

Supporting Information Available: Figures S1 and S2 displaying the fluorescence response of CZ1 and CZ2 over a zinc concentration range following excitation at 445 or 505 nm. This material is available free of charge via the Internet at http://pubs.acs.org.

IC048789S